CIRRUS CLOUD REMOTE SENSING FROM SPLIT WINDOW AND 6.7μm

Toshiro Inoue and Yuzo Mano
Meteorological Research Institute / JMA, Tsukuba, Ibaraki, Japan

1. INTRODUCTION

Cirrus clouds are thought to play an important role in global-climate feedbacks. Whether a cirrus cloud causes radiative heating or cooling to the earth-atmosphere system depends on the cloud height, sizes and shapes of ice particles. However, we little know about the cirrus cloud climatology. Satellite remote sensing is considered an effective tool for observing cloud radiative properties, but the cirrus cloud (which is composed of ice) are difficult to detect. Thus far, the number of cirrus cloud detection algorithms using satellite observations is very small. Single-channel infrared methods are of limited utility due to the semi-transparency of many cirrus. Other investigators use visible and 3.7μm data; however, these algorithms cannot be used equally during both day and night.

Inoue(1985) first demonstrated the usage of split window data (11μm and 12μm in combination), which can be used equally both day and night, in detecting cirrus clouds. In the study, cirrus cloud is characterized as the cloud of which brightness temperature difference (BTD) between the split window is larger than the BTD over the near-by cloud free area. Some theoretical and observational studies to use the split window in retrieving cirrus cloud properties were followed by some authors (e.g., Wu (1987), Prabhakara et al. (1988), Parol et al. (1991), King et al.(1992)). The use of 6.7μm and 11μm for the study of semi-transparent clouds is first proposed by Szejwach(1982) and followed by some works (e.g., Pollinger and Wendling (1984), Schmetz et al.(1993)). These two channels are effective in retrieving cirrus cloud temperature.

Corresponding author address: Toshiro Inoue, Meteorological Research Institute/JMA, 1-1 Nagamine, Tsukuba Ibaraki 305-0052, Japan; e-mail:tinoue@mri-jma.go.jp

In this study, an algorithm to retrieve optical thickness and effective radius of cirrus clouds using split window data and 6.7μm has been developed and applied to GOES-9 observations and diurnal variability of optical properties of cirrus cloud have been studied. The advantage of using these infrared channels is equal quality in retrievals for both day and night.

2. CIRRUS CLOUD AND SPLIT WINDOW (11μm and 12μm)

Simulated brightness temperatures are computed from the radiative transfer equation for given optical thickness and cirrus cloud temperatures. Vertical temperature and water vapor profiles are taken from the US standard tropical atmosphere. Cloud droplets are assumed to be both spherical and hexagonal column. The drop sizes are characterized by modified gamma distribution. Complex indices by Warren (1984) are used. Fluxes are computed by the 8-stream method. In this study, radiance for the split window are computed at 10.7μm and 11.8μm.

Figure 1 shows computed brightness temperatures (TBB) and brightness temperature differences {BTD=TBB(10.7μm)-TBB(11.8μm)} for effective radius of 11.1μm sphere and 40μm-16μm hexagonal column, with changing cloud temperature and cloud optical thickness. The solid curve indicate spherical particles, while thin curve indicate hexagonal column. The difference of ice particle shape is not so large for this wavelength region. In this computation water vapor absorption was neglected. Figure 2 shows the TBB-BTD diagram for -50℃ cirrus cloud for three different effective radius of 10μm, 20μm and 30μm with changing the optical thickness.

These figures indicate cirrus clouds are characterized as clouds whose BTD are larger than that of cloud free(zero optical thickness) which the BTD indicates the total water vapor amount. Further theses figures demonstrate the BTD dependence on effective radius, cloud

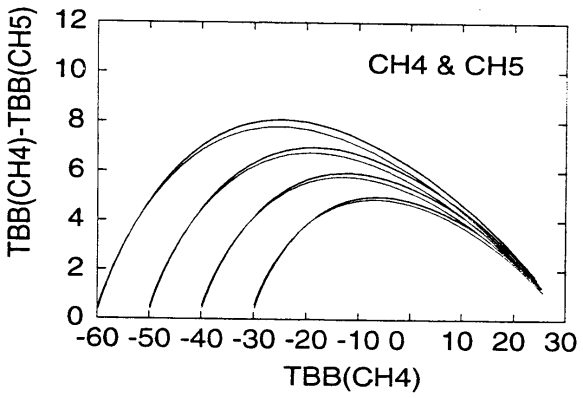

Figure 1 Computed TBB and BTD for sphere and hexagonal column with changing cirrus cloud temperature and optical thickness.

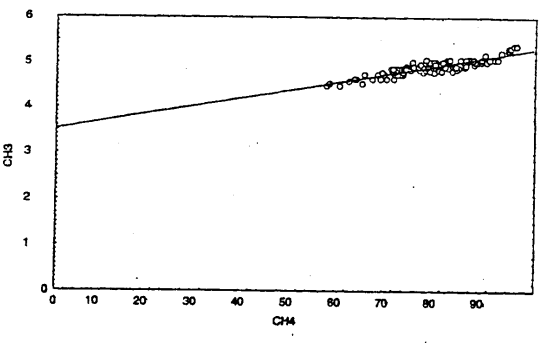

Figure 3a Scatter plot of 11μm and 6.7μm radiances for cirrus anvil.

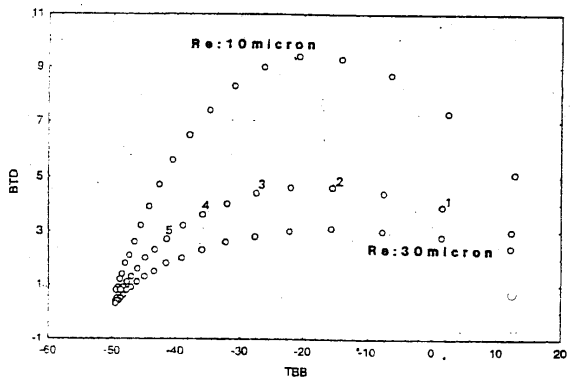

Figure 2 Computed TBB and BTD for -50C cirrus cloud with changing effective radius and optical thickness.

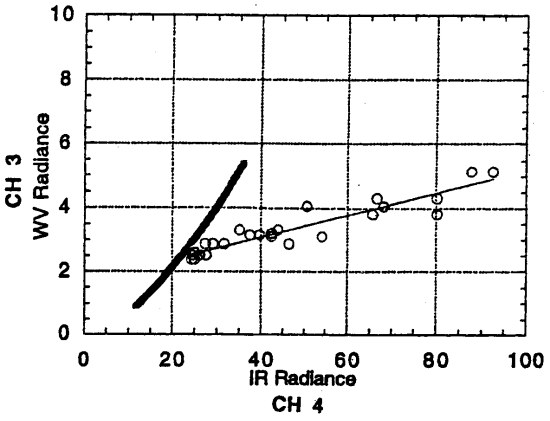

Figure 3b Scatter plot 11μm and 6.7μm for another cirrus cloud with curve for black-body cloud.

temperature and optical thickness. We also understand the possibility of retrieving cloud properties using TBB and BTD by assuming one parameter of either optical thickness, cloud temperature, or cloud effective radius. ISCCP assumes the effective radius, while in this study, cirrus cloud temperatures are estimated from 11μm and 6.7μm observations.

The table of TBB and BTD is constructed in advance for various cloud temperatures, optical thickness, effective radii and satellite zenith angles using the standard tropical atmosphere or global analysis data from Japan Meteorological Agency (JMA). The table is used to find an optimal optical thickness and effective radius from satellite observation of TBB and BTD.

3. CIRRUS CLOUD TEMPERATURE RETRIEVAL FROM 11μm AND 6.7μm

Based on the idea of Szejwach (1982), linearity of radiance at 11μm and 6.7μm is studied for cirrus clouds over the central Pacific using GOES-9 data. Figure 3a shows an example of scatter plot of 11μm and 6.7μm radiance for cirrus anvils associated with deep convection. Cirrus cloud pixels of 10 by 10, which belong to same cirrus anvil cloud selected by subjective inspection of the BTD and TBB images, are used to construct the plots. Generally, we can see good linearity between the two radiance for cirrus clouds. The bold curve in the Figure 3b (similar

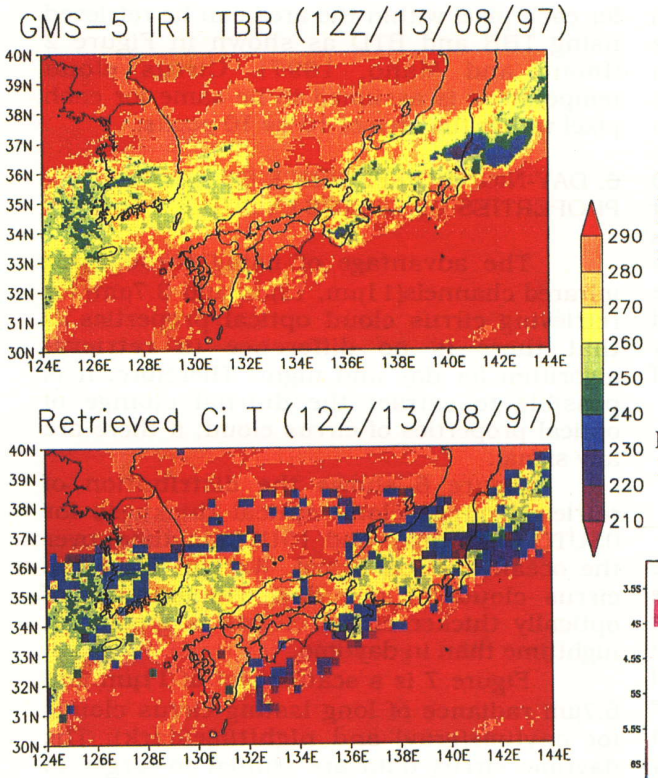

Figure 4 GMS-5 TBB(top, a), and retrieved cirrus cloud temperature(bottom, b).

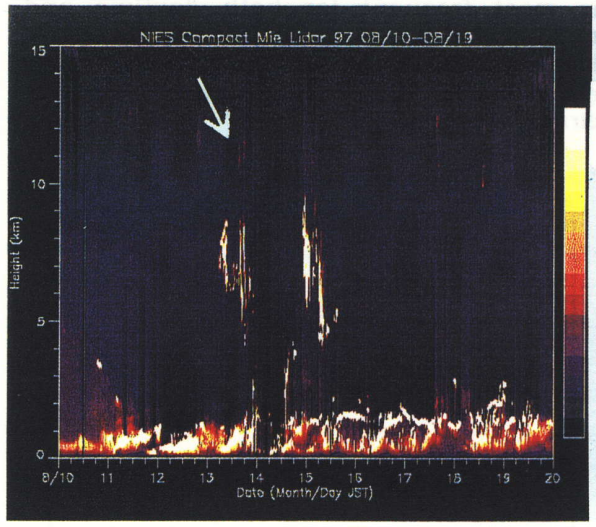

Figure 5a Mie lidar observation at NIES during 10-20 August, 1997.

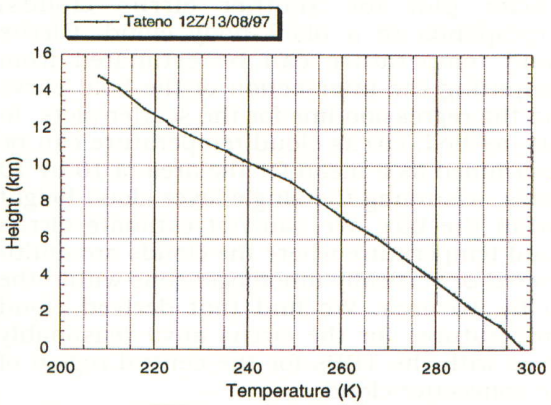

Figure 5b Radiosonde observation at Tateno 12 UTC on 13 August, 1997.

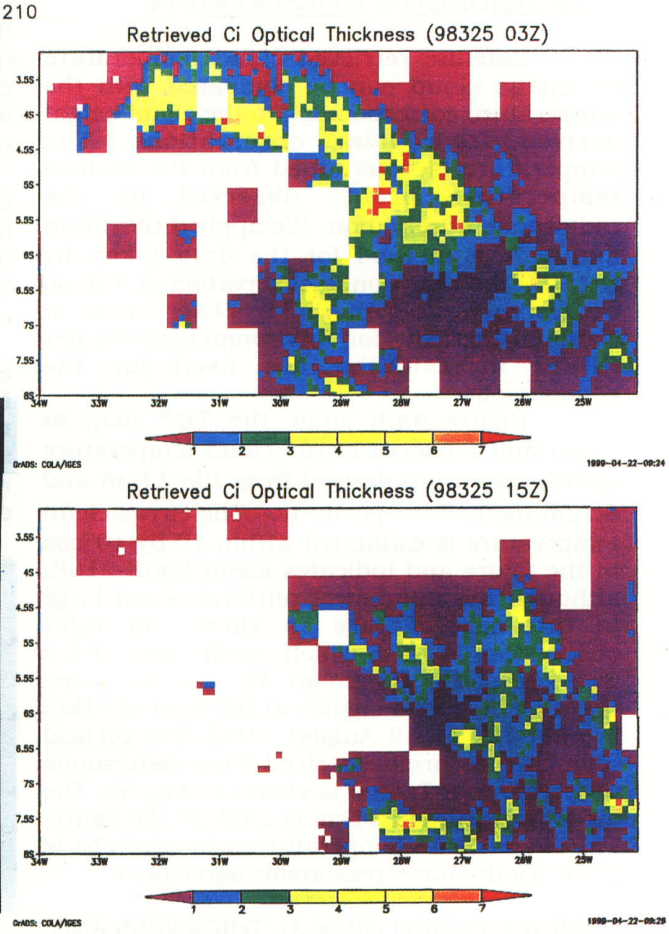

Figure 6 Retrieved cirrus cloud optical thickness for 03UTC (nighttime) and 15UTC (daytime) over the ocean east off Brazil.

scatter plot for another cirrus clouds) corresponds to a black-body cloud. Cirrus cloud temperature can be estimated from computing the intersection of the bold curve and the regression line for the scatter plots. In this method, cirrus cloud temperature can be determined as a mean for the area of 10 by 10 pixels, assuming the single layer cloud height within the box. We can not estimate cirrus cloud temperature where the clouds are multi-layered or vertically inhomogeneous within the 10 by 10 area. We find that derived cloud temperatures for the cirrus anvil reasonably agree with the TBBs for the central region of the convective cloud.

4. COMPARISON BETWEEN RETRIEVED CIRRUS CLOUD TEMPERATURE AND LIDAR/RADIOSONDE OBSERVATION

Satellite retrieved cloud temperature for cirrus cloud can be compared with the temperature corresponding to the cloud height derived from lidar observations. The temperature is determined from the vertical temperature profile observed by the radiosonde observation. We applied the 11μm and 6.7μm method for the data taken by GMS-5. The radiosonde observation at Tateno in Tsukuba and the lidar observation at National Institute for Environmental Studies (NIES) in Tsukuba are used for the comparison.

Figure 4a,b show the TBB map at 11μm and retrieved cirrus cloud temperature distribution map derived from the 11μm and 6.7μm method, respectively. The cirrus cloud temperature is estimated within 10 by 10 box in the figure and indicates about 240K-210K, although the number of retrieval is not large in this case. Figure 5a shows the lidar observation at NIES which can be seen at the web site of Dr. Sugimoto. We can see some slight cirrus cloud signals at the level of 11km around 12Z on 13 August, 1997. The vertical temperature profile derived from radiosonde observation at Tateno is shown in Fig. 5b. The air temperature at 11km is 235K in the figure. The cirrus cloud temperature near Tsukuba is 230K. Both shows reasonable agreement.

5.CIRRUS CLOUD OPTICAL THICKNESS AND EFFECTIVE RADIUS RETRIEVAL FROM SPLIT WINDOW

Once mean cirrus cloud temperature is determined for the area using the 11μm and 6.7μm, optical thickness and effective radius for each pixel within the area can be retrieved using TBB and BTD as shown in Figure 2 (Inoue and Mano, 1997). Cirrus cloud temperature is assumed to be same for each pixel within the area of 10 by 10 pixels.

6. DAY-NIGHT DIFFERENCE OF OPTICAL PROPERTIES OF CIRRUS CLOUD

The advantage of using these three infrared channels(11μm, 12μm and 6.7μm) for retrieving cirrus cloud optical properties is that there is no difference in retrieval algorithm for day and night. Therefore, it is possible to extract the diurnal change of optical properties of cirrus cloud, if there are any signal.

Figure 6 shows the distribution of retrieved cirrus cloud optical thickness for 03UTC (nighttime) and 15UTC(daytime) over the ocean east off Brazil. We can trace the cirrus cloud for one day. The number of optically thicker cirrus clouds is greater at nighttime than in daytime.

Figure 7 is a scatter plot of 11μm and 6.7μm radiance of long lasting cirrus clouds for daytime(gray) and nighttime(dark). The daytime cirrus data are shifted to larger in 6.7μm axis, which means that the retrieved cloud temperature is warmer.

Figure 8 shows histogram of retrieved effective radius. The effective radius of 30μm is most frequent for both daytime and nighttime. Although the distribution pattern is similar, the relative frequency for effective radius smaller than 10μm is larger for daytime cirrus.

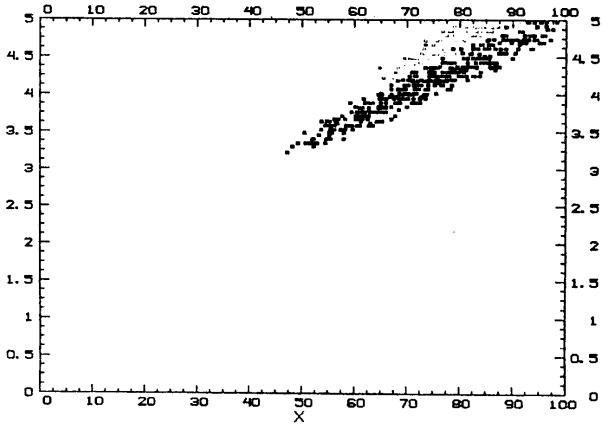

Figure 7 Scatter plot of 11μm and 6.7μm radiance of cirrus clouds for daytime(gray) and nighttime(dark).

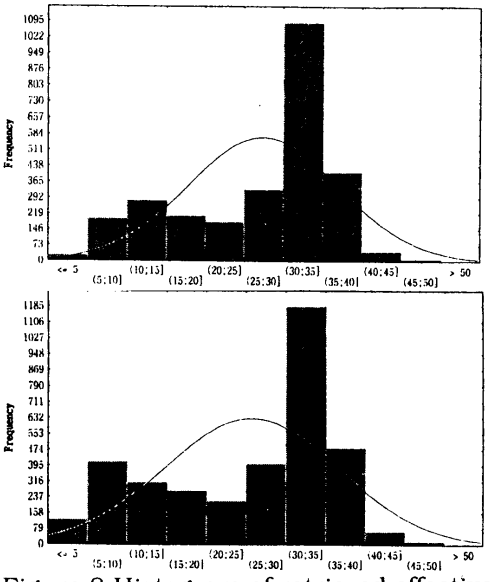

Figure 8 Histogram of retrieved effective radius for day(bottom) and night(top).

7. SUMMARY

A method of retrieving cirrus cloud optical thickness and mean effective radius and cloud temperature using three infrared data of split window(11μm, 12μm) and 6.7μm has been developed and applied to GOES-9 split window data. First, cloud temperature was estimated from 11μm and 6.7μm data, then optical thickness and effective radius are retrieved from split window. Case studies show reasonable cirrus cloud temperatures which coincide with the temperature at the core of deep convection and nearby lidar/ radiosonde observation.

The advantage of using these infrared channels is equal quality in retrievals for both day and night. Although the night-day difference of cirrus cloud optical properties is small, some long lasting cirrus clouds show that the temperature tend to be colder, the optical thickness tend to be larger, and the effective radius tend to be larger at night.

The cirrus cloud radiative effect on heating or cooling to the earth-atmosphere system depends on the cloud height, sizes and shapes of ice particles. The satellite algorithm is essential for this kind of study and is required for validation by cloud profiling radar/lidar on the same satellite.

8. References

Inoue, T. 1985: On the temperature and effective emissivity determination of semi-transparent cirrus clouds by bispectral measurements in the 10μm window region. J. Meteor. Soc. Japan. 63, 88-98.

Inoue,T. and Y.Mano,1997:Retrieval of cirrus cloud properties from split window and 6.7μm measurements. Proceedings of the 7th ARM science team meeting

King, M. D., Y.J. Kaufman, W.P. Menzel, and D. Tanr, 1992: Remote sensing of cloud, aerosol and water vapor properties from Moderate Resolution Imaging Spectrometer (MODIS). IEEE Trans. Geoscience and Remote Sensing, 30, 2-27.

Manabe, S., and R.F. Strickler, 1964: Thermal equilibrium of the atmosphere with a convective adjustment. J.Atmos.Sci., 21, 361-385.

Parol, F., J.C. Buriez, G. Brogniez and Y. Fouquart,1991: Information content of AVHRR channels 4 and 5 with respect to the effective radius of cirrus cloud particles. J. Appl. Meteor., 30, 973-984.

Pollinger, W. and P. Wendling, 1984: A bispectral method for the height determination of optically thin ice clouds., Contrib. Atmos. Phys., 57, 269-281.

Prabhakara, C., R.S. Fraser, G. Dalu, M.L.C. Wu, R.J. Curran, and T. Styles, 1988: Thin cirrus clouds: seasonal distribution over oceans deduced from Nimbus-4 IRIS. J. Appl. Meteor., 27, 379-399.

Schmetz, J., K. Holmlund, J. Hoffman, B. Strauss, B Mason, V. Gaertner, A. Koch and L.V.D. Berg, 1993: Operational cloud-motion winds from Meteosat infrared images, J. Appl. Meteor., 32, 1206-1225.

Szejwach, G., 1982: Determination of semi-transparent cirrus cloud temperature from infrared radiances: Application to METEOSAT. J. Appl. Meteor., 21, 384-393.

Warren, S.G., 1984: Optical constants of ice from the ultraviolet to the microwave. Appl. Opt., 23, 1206-1225.

Wu, M.C., 1987: A method of remote sensing the emissivity, fractional cloud cover, and cloud top temperature of high-level thin clouds. J. Climate Appl. Meteor., 26, 225-233